

Classical Model of Extrinsic Ferromagnetic Resonance Linewidth in Ultrathin Films

Robert D. McMichael, *Member, IEEE*, and Pavol Krivosik

Abstract—This paper describes a classical version of the two-magnon model of ferromagnetic resonance linewidth in inhomogeneous magnetic thin films. The ferromagnetic resonance line broadening due to inhomogeneity is described in terms of film properties and the statistical properties of the inhomogeneity. Analytical results for the case of ultrathin films in the limit of zero damping are compared with numerical results computed with finite damping.

Index Terms—Ferromagnetic resonance, linewidth, magnetization dynamics.

I. INTRODUCTION

COUPLING between the magnetization and the thermal bath in ferromagnets and ferrimagnets is responsible for damping, the process that allows the magnetization to lose energy and approach equilibrium [1]–[9]. The same coupling is also responsible for thermally driven fluctuations of the magnetization [3], [10]–[14]. Both damping and fluctuations are important for the behavior of magnetic devices, especially heads and media used in magnetic information storage.

In the time domain, ferromagnetic resonance (FMR) appears as a ringing of the magnetization [15], while in the frequency domain, ferromagnetic resonance appears as a maximum in the transverse susceptibility at a frequency matching the precession frequency. The ferromagnetic resonance linewidth, which is the width of this susceptibility peak, provides a convenient avenue for measuring damping in magnetic materials, with the possible caveat that it is not always clear how to identify the effects of inhomogeneity of the sample in the measured linewidth. For example, one might assume that the dynamics of the magnetization \mathbf{M} are correctly described by the Landau–Lifshitz–Gilbert (LLG) equations of motion

$$\frac{d\mathbf{M}}{dt} = -|\gamma|\mathbf{M} \times \mathbf{H}_{\text{eff}} + \alpha \frac{\mathbf{M}}{M_s} \times \frac{d\mathbf{M}}{dt} \quad (1)$$

where $|\gamma| = \mu_0 g \mu_B / \hbar = 2.21 \times 10^5$ m/(As) is the gyromagnetic ratio, \mathbf{H}_{eff} is an effective field that depends on the mag-

netization, applied fields, and material parameters, and α is the LLG damping parameter.

In the typical case of weak damping when the magnetization is close to its equilibrium direction, (1) describes damped precession of the magnetization around the equilibrium direction at a frequency determined by \mathbf{H}_{eff} [16]. As described in more detail below, for special cases where the magnetization and applied field are parallel, the LLG equations of motion (1) lead to a full width of the resonance

$$\Delta H = \frac{2\alpha\omega_0}{|\gamma|}. \quad (2)$$

This expression is appropriate for an experiment where the spectrometer drives the magnetization at angular frequency ω_0 and the transverse susceptibility is measured as a function of applied field. There are other possible phenomenological descriptions of damping that lead to other expressions for the linewidth [1], [16], but for some nominally uniform films, the linewidth is well described by the LLG form of damping [17].

Regardless of the phenomenological description or physical mechanism of damping, an increase in linewidth can be expected as a consequence of sample inhomogeneity. The inhomogeneity may arise from a wide variety of microstructural origins including magnetocrystalline anisotropy in a polycrystalline sample, magnetostriction coupled with nonuniform stresses, surface anisotropy with film thickness variations, and step/edge anisotropy. Given that inhomogeneity exists to some degree in all experimental samples, interpretation of linewidth data solely as a damping phenomenon will result in an artificially high estimate of the damping. It is clear that good models of inhomogeneous line broadening in ferromagnetic resonance are needed to compensate for possible inhomogeneity effects in measurements of damping.

Recent modeling of linewidth in thin films [18] supports earlier work in bulk ferrites [19] that indicates that the degree of line broadening caused by inhomogeneity depends on the relative strengths of the inhomogeneous effective field and the interactions. In one limit, the inhomogeneities are much stronger than the exchange and dipolar interactions between different parts of a film. In this case, the simplest model treats the inhomogeneous film as a collection of noninteracting regions where the magnetization will resonate at a frequency/field combination that is determined by the local properties of the film. The resonance becomes a superposition of resonances from different regions, and the inhomogeneity line shape is a rather direct measurement of the distribution in local effective fields [20]–[25]. These “local resonance” models of linewidth have been successful in describing the linewidth in a number of thin-film

Manuscript received June 13, 2003; revised October 8, 2003. The work of R. D. McMichael was supported by the National Institute of Standards and Technology (NIST) Nanotechnology Program. The work of P. Krivosik was supported by a postdoctoral fellowship from the National Science Foundation (DMR-0108797) and by the U. S. Office of Naval Research (N00014-03-1-0070).

R. D. McMichael is with the National Institute of Standards and Technology, Gaithersburg, MD 20899 USA (e-mail: rmc michael@nist.gov).

P. Krivosik is with the Department of Physics, Colorado State University, Fort Collins, CO 80523 USA, on leave from the Faculty of Electrical Engineering and Information Technology, Slovak University of Technology, 81219 Bratislava, Slovakia.

Digital Object Identifier 10.1109/TMAG.2003.821564

cases [25]–[28]. In particular, when the inhomogeneities have the effect of a varying applied field, the local resonance model linewidth for $\mathbf{H} \parallel \mathbf{M}_s$ becomes

$$\Delta H = \Delta H_0 + \frac{2\alpha\omega}{|\gamma|}. \quad (3)$$

In a number of measurements of the frequency dependence of linewidth in thin films, the data is reasonably well described by a linear relationship of this type [17], [26], [29]–[34].

In the opposite limit, the exchange and dipolar interactions are very strong, forcing the magnetization to precess nearly uniformly and effectively smoothing the inhomogeneity over the film area. The two-magnon model of linewidth addresses this case. The magnetization is treated in terms of spin waves, the normal modes of the uniform film, or in the terminology of quantum mechanics, magnons. The usual picture of the two-magnon model is that inhomogeneities introduce weak interactions between the spin-wave modes that allow the energy of the uniform precession to leak into a number of other modes, providing an effective damping of the uniform mode. Alternatively, the effect of the inhomogeneity may be regarded as a mixing of the eigenmodes of the uniform film in a way that distributes the FMR intensity over a number of eigenmodes, resulting in an FMR peak composed of a number of overlapping resonances [18].

Typically, the two-magnon model is treated in a lowest-order perturbation approach, treating the inhomogeneity as a small quantity. Higher order approaches include consideration of the effects of inhomogeneity on the spin-wave density of states [35], [36] and a recursive method described by Schlömann [19].

The purpose of this paper is to describe the two-magnon model for ultrathin films in classical terms, giving analytical formulas for the case of ultrathin films in the limit of zero damping, and numerical results for finite damping. To accommodate high-magnetization films, we include all the effects of the precessional ellipticity. Early classical treatment of the two-magnon model was given by Clogston [37] for bulk materials, and more recently for case of a thin film with in-plane magnetization by Arias and Mills [38], [39]. Quantum mechanical two-magnon models for thick films have been published by Sparks [40] and Hurben and Patton [41].

In Section II, the spin-wave normal modes of a uniform ultrathin film are reviewed. Section III includes a brief description of the quantum mechanical two-magnon model. Section IV describes the excitation of spin waves and their interaction with the uniform precession to produce an effective damping. Analytical results for special cases are given in Section V, and example calculations are given in Section VI.

II. SPIN-WAVE NORMAL MODES

Using the coordinate system shown in Fig. 1, the magnetization is written as $\mathbf{M} = M_s \hat{\rho} + m_\theta(\mathbf{r}) \hat{\theta} + m_\phi(\mathbf{r}) \hat{\phi} = M_s \hat{\rho} + \mathbf{m}(\mathbf{r})$, where \mathbf{r} is a two-dimensional (2-D) vector in the plane of the film. The radial unit vector $\hat{\rho}$ is chosen to lie along the spatially averaged equilibrium magnetization direction, and $\hat{\theta}$ and $\hat{\phi}$ are chosen to lie along the major axes of the ellipse traced out by the uniform precession. The magnetization is assumed

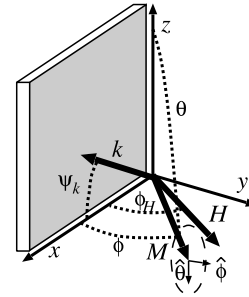


Fig. 1. Coordinate system used to describe the magnetization, wave vectors, and the applied field. The spin-wave wave vectors \mathbf{k} lie in the x - z plane, and the precession of the magnetization traces an ellipse in the θ - ϕ plane around a spatially averaged equilibrium direction in the x - y plane.

to be independent of y through the thickness d of the film. Fourier expansions of spatially dependent quantities will use the convention

$$b(\mathbf{r}) = \int \frac{d\mathbf{k}}{(2\pi)^2} b(\mathbf{k}) e^{i\mathbf{k}\cdot\mathbf{r}} \quad (4)$$

and $\exp(i\omega t)$ time dependence is assumed for all dynamic quantities.

Expressions for \mathbf{H}_{eff} , the effective field acting on the magnetization, are needed to describe the linear dynamics of the magnetization near its equilibrium direction. Because the effective field \mathbf{H}_{eff} enters the equations of motion (1) only in a cross product $\mathbf{M} \times \mathbf{H}_{\text{eff}}$, the only important components of \mathbf{H}_{eff} are perpendicular to \mathbf{M} , i.e., components in the θ - ϕ plane. Calculation of the θ and ϕ components of the field is most easily achieved by expanding the energy of the magnetization in terms of m_θ and m_ϕ , using the constraint $M_\rho^2 + m_\theta^2 + m_\phi^2 = M_s^2$ to eliminate M_ρ . The effective field is then proportional to the gradient of the local energy density $E(\mathbf{r})$

$$\mathbf{H}_{\text{eff}}(\mathbf{r}) = -\frac{1}{\mu_0} \nabla_{\mathbf{m}(\mathbf{r})} E(\mathbf{r}). \quad (5)$$

Interactions, particularly exchange interactions and dipole-dipole interactions, are important for the description of spin waves, and ultimately for the behavior of the inhomogeneous film. Interactions may be described in terms of a field at a particular location in a magnetic material that depends on the magnetization at another location. For nonlocal interactions in a uniform film, we consider the case where the kernel tensor \mathbf{G} exhibits translational invariance

$$\mathbf{H}_{\text{eff}}(\mathbf{r}) = \int d\mathbf{r}' \mathbf{G}(\mathbf{r} - \mathbf{r}') \mathbf{m}(\mathbf{r}'). \quad (6)$$

Important examples of such nonlocal interactions are the dipolar, or magnetostatic interaction and the exchange interaction. Note that local energy densities such as Zeeman or magnetocrystalline anisotropy that have local effective fields can be described by the special case where \mathbf{G} is proportional to $\delta(\mathbf{r} - \mathbf{r}')$.

Using translational invariance, the Fourier components of the field in a uniform film can be written as

$$\mathbf{H}(\mathbf{k}) = -\mathbf{h}_{\mathbf{k}} \mathbf{m}(\mathbf{k}). \quad (7)$$

Using the coordinate system in Fig. 1, the elements of the normalized stiffness field tensor $h_{\mathbf{k}}$ are given by [18], [42], [43]

$$h_{\theta\theta,\mathbf{k}} = M_s^{-1} [H_i + Dk^2 + M_s(1 - N_k) \sin^2 \psi_k] \quad (8a)$$

$$h_{\phi\phi,\mathbf{k}} = M_s^{-1} [H_i + Dk^2 + M_s N_k \cos^2 \phi + M_s(1 - N_k) \sin^2 \phi \cos^2 \psi_k] \quad (8b)$$

$$h_{\theta\phi,\mathbf{k}} = M_s^{-1} [M_s(1 - N_k) \cos \psi_k \sin \psi_k \sin \phi] \quad (8c)$$

$$h_{\phi\theta,\mathbf{k}} = h_{\theta\phi,\mathbf{k}} \quad (8d)$$

where $Dk^2 = (2A/\mu_0 M_s)k^2$ is the exchange field for a spin wave with wave vector \mathbf{k} under the assumption that the wavelengths of interest are much larger than the lattice spacing where A is the exchange stiffness, and $H_i = H \cos(\phi - \phi_H) - M_s \sin^2 \phi$ is the ‘‘internal field’’ consisting of the component of H parallel to the magnetization and the static part of the demagnetization field. The k -dependent demagnetization factor for a film of thickness d is given by

$$N_k = \frac{1 - e^{-kd}}{kd} \quad (9)$$

under the approximation that the magnetization does not vary significantly across the thickness of the film [44].

The susceptibility tensor $\chi_{\mathbf{k}}(\omega)$ can be obtained from the linearized LLG equations of motion (1). For an applied field with spatial frequency \mathbf{k} and angular frequency ω , the transverse susceptibility tensor is given by

$$\chi_{\mathbf{k}}(\omega) = \frac{1}{Z_{\mathbf{k}}} \begin{bmatrix} h_{\phi\phi,\mathbf{k}} + \frac{i\alpha\omega}{\omega_M} & -h_{\theta\phi,\mathbf{k}} + \frac{i\omega}{\omega_M} \\ -h_{\phi\theta,\mathbf{k}} - \frac{i\omega}{\omega_M} & h_{\theta\theta,\mathbf{k}} + \frac{i\alpha\omega}{\omega_M} \end{bmatrix} \quad (10a)$$

$$Z_{\mathbf{k}} = h_{\theta\theta,\mathbf{k}} h_{\phi\phi,\mathbf{k}} - h_{\theta\phi,\mathbf{k}} h_{\phi\theta,\mathbf{k}} - (1 + \alpha^2) \left(\frac{\omega}{\omega_M} \right)^2 + i\alpha \left(\frac{\omega}{\omega_M} \right) (h_{\theta\theta,\mathbf{k}} + h_{\phi\phi,\mathbf{k}}) \quad (10b)$$

where $\omega_M = |\gamma| M_s$.

The imaginary part of (10) describes magnetization damping, and the particular form follows from our choice of Gilbert damping in (1). Other descriptions of damping produce susceptibility expressions with different damping characteristics [16], but the basic features, including the dispersion relation, are nearly independent of damping.

The dispersion relation is obtained by noting that the $|Z_{\mathbf{k}}|$ is minimum and susceptibility is in resonance when

$$\omega = \omega_{\mathbf{k}} \equiv \frac{\omega_M}{\sqrt{1 + \alpha^2}} [h_{\theta\theta,\mathbf{k}} h_{\phi\phi,\mathbf{k}} - h_{\theta\phi,\mathbf{k}} h_{\phi\theta,\mathbf{k}}]^{1/2}. \quad (11)$$

When a spin wave is driven ‘‘on resonance’’ by a field with wave vector \mathbf{k} and $\omega = \omega_{\mathbf{k}}$, $Z_{\mathbf{k}}$ becomes pure imaginary, and for small α the magnetization lags the driving field by $\pi/2$.

The dispersion relation is important for a number of reasons, but its primary importance here is that it encapsulates the interactions in the film. An example dispersion relation for a 50-nm-thick film of $\text{Ni}_{80}\text{Fe}_{20}$ is plotted in Fig. 2(a). Without either exchange or magnetostatic interactions, the dispersion relation would be a flat horizontal line. Note that there is a set of wave vectors describing spin waves with $\omega_0 \approx \omega_{\mathbf{k}}$ displayed in Fig. 2(b). These *degenerate spin waves* play an important role in the effect of inhomogeneities on the uniform precession.

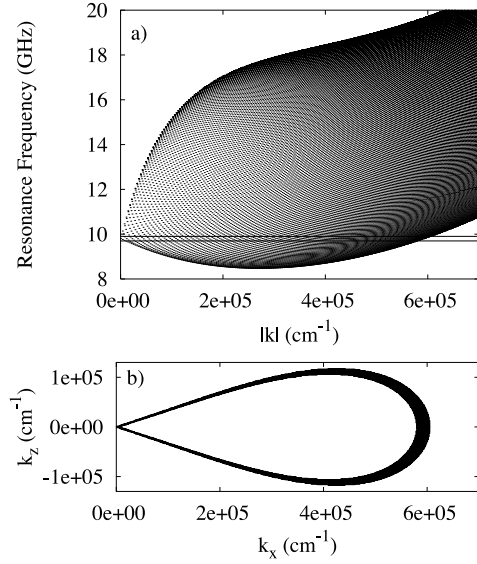


Fig. 2. (a) Spin-wave dispersion relation for a 50-nm-thick Permalloy film with 101 mT applied in plane. The $\mathbf{k} = 0$ FMR frequency is 9.8 GHz. For any value of $|\mathbf{k}|$, the highest frequencies are for $\mathbf{k} \perp \mathbf{M}_s$ and the lowest frequencies are for $\mathbf{k} \parallel \mathbf{M}_s$. The horizontal lines bound a set of nearly degenerate spin waves having $|\omega_{\mathbf{k}} - \omega_0| < 2\pi \cdot 100$ MHz. (b) Half of the wave vectors of nearly degenerate spin waves. Only $k_x > 0$ is plotted.

III. QUANTUM TWO-MAGNON THEORY

The quantum mechanical description of the two-magnon model has been developed and used by many authors [41], [42], [45]–[48], and there are several good reviews available [49]–[51], so only a brief description will be given here.

In the quantum mechanical two-magnon model, the spin-wave normal modes are described by raising and lowering operators $a_{\mathbf{k}}^\dagger$ and $a_{\mathbf{k}}$. When an inhomogeneous energy term $E'(\mathbf{r}, m_\theta, m_\phi)$ is added, and m_θ and m_ϕ are expanded in terms of $a_{\mathbf{k}}^\dagger$ and $a_{\mathbf{k}}$, the perturbed Hamiltonian can be put into the form

$$\mathcal{H} = \hbar\omega_0 a_0 a_0^\dagger + \hbar \sum_{\mathbf{k}} \omega_{\mathbf{k}} a_{\mathbf{k}} a_{\mathbf{k}}^\dagger + \sum_{\mathbf{k}} A_{\mathbf{k}} a_{\mathbf{k}}^\dagger a_0 + A_{\mathbf{k}}^* a_0^\dagger a_{\mathbf{k}} \quad (12)$$

where the first two terms describe the linear dynamics of the spin waves in a uniform film, and the coefficients $A_{\mathbf{k}}$ arise from the perturbation energy E' . Only terms involving the $\mathbf{k} = 0$ magnon are kept in the perturbation part of the Hamiltonian. The two-magnon terms in the Hamiltonian containing $a_{\mathbf{k}}^\dagger a_0$ describe scattering where $\mathbf{k} \neq 0$ magnons are created and $\mathbf{k} = 0$ magnons are annihilated. The effective damping rate of the $\mathbf{k} = 0$ magnons is the sum of the scattering rates to each of the other magnon states, and perturbation theory yields the two-magnon linewidth

$$\Delta\omega = \frac{2\pi}{\hbar} \sum_{\mathbf{k}} |A_{\mathbf{k}}|^2 \delta(\hbar\omega_0 - \hbar\omega_{\mathbf{k}}). \quad (13)$$

Three features of (13) are noted for comparison with the classical result described in Section IV. The effective linewidth is a sum over magnon states, the sum is restricted to degenerate magnons, and the linewidth depends on the square of the inhomogeneity strength.

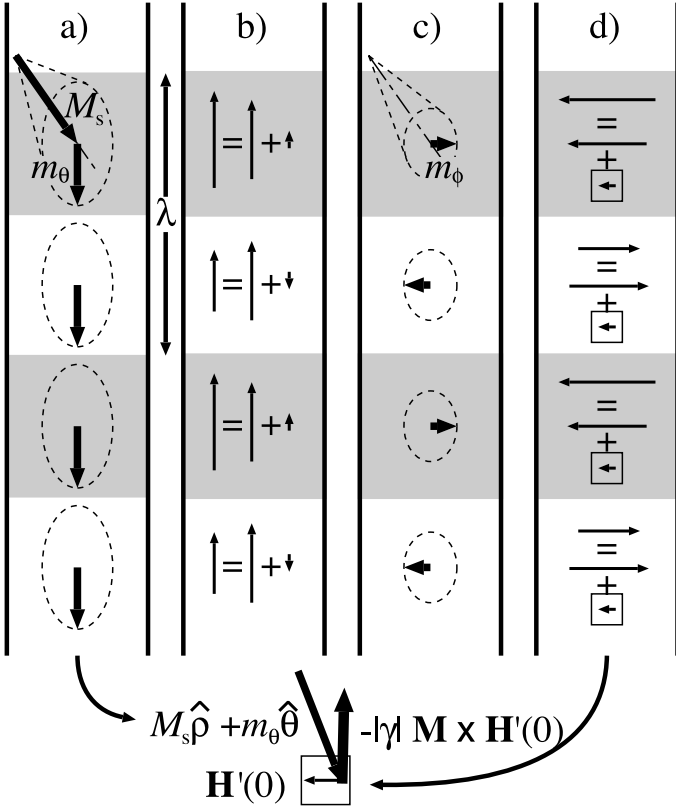


Fig. 3. Illustration of spin-wave magnetization (heavy arrows) and resulting effective fields (light arrows) in an inhomogeneous material with stronger anisotropy in the shaded regions. The uniform magnetization of the $k = 0$ mode [panel a], (20) precesses counterclockwise with angular frequency ω_0 and results in a mostly uniform effective field with a small $k = 2\pi/\lambda$ component [panel b], (21)]. The $k = 2\pi/\lambda$ component of the effective field in b) drives a spin wave with magnetization [panel c], (22)] that lags its driving field by $\pi/2$ when $\omega_k = \omega_0$. The effective field resulting from the $k = 2\pi/\lambda$ spin wave results in a mostly sinusoidal field [panel d], (23)] with a small uniform component, $\mathbf{H}'(0)$ (boxed) that produces a torque that decreases the amplitude of the $k = 0$ spin-wave magnetization.

IV. CLASSICAL TWO-MAGNON MODEL

In this section, the spin-wave susceptibility (10) is used to describe the behavior of the magnetization in a weakly inhomogeneous film. Briefly, the interaction of the uniform precession with inhomogeneities creates a nonuniform field that excites spin waves, as illustrated in Fig. 3. The interaction of the nonuniform spin-wave magnetization with the inhomogeneities generates an effective field with a uniform component that acts on the uniform precession. The spin-wave susceptibility is complex, so the uniform precession experiences a dissipative field that is out of phase with the magnetization, creating an effective damping.

The classical approach to the two-magnon damping process described below parallels the quantum mechanical approach, but has two advantages. First, damping of the magnon modes replaces the delta function in (13) with a finite width peak that can be changed in a natural way to model different amounts and phenomenological models of damping. It is shown below that the two-magnon linewidth has a significant dependence on the damping. In fact, self-consistent schemes for calculating higher order effects rely on the dependence of the effective spin-wave damping on the two-magnon linewidth [19]. Second, results

are given in terms of magnetizations and fields rather than Hamiltonian coefficients. This property simplifies the process of calculating the two-magnon linewidth from particular inhomogeneity models.

Inhomogeneity is introduced as a local, inhomogeneous, perturbation energy density $E'(\mathbf{r}, m_\theta, m_\phi)$. Nonlocal dipolar effects of variations in M_s , especially pits and holes, have been treated quantum mechanically elsewhere [40], [41], [51]. Here, and in what follows, primed quantities are quantities that describe the inhomogeneity. For each point in the film, the perturbation energy density can be expanded in terms of m_θ and m_ϕ

$$E'(\mathbf{r}, m_\theta, m_\phi) = E'_0(\mathbf{r}, 0, 0) + \frac{1}{M_s} \left[\frac{\partial E'(\mathbf{r})}{\partial \theta} m_\theta(\mathbf{r}) + \frac{\partial E'(\mathbf{r})}{\sin \theta \partial \phi} m_\phi(\mathbf{r}) \right] + \frac{\mu_0}{2} [h'_{\theta\theta}(\mathbf{r}) m_\theta(\mathbf{r})^2 + h'_{\phi\phi}(\mathbf{r}) m_\phi(\mathbf{r})^2 + 2h'_{\theta\phi}(\mathbf{r}) m_\theta(\mathbf{r}) m_\phi(\mathbf{r})]. \quad (14)$$

The linear terms in the second line of (14) provide inhomogeneous static fields, which drive magnetization ripple [44]. The effects of ripple will not be considered further in this paper.

The second-order terms in (14) involve normalized perturbation stiffness fields h' that are given by

$$h'_{\theta\theta}(\mathbf{r}) = \frac{1}{\mu_0 M_s^2} \frac{\partial^2 E'(\mathbf{r})}{\partial \theta^2} \quad (15a)$$

$$h'_{\phi\phi}(\mathbf{r}) = \frac{1}{\mu_0 M_s^2} \left[\frac{1}{\sin^2 \theta} \frac{\partial^2 E'(\mathbf{r})}{\partial \phi^2} + \frac{\cos \theta}{\sin \theta} \frac{\partial E'}{\partial \theta} \right] \quad (15b)$$

$$h'_{\theta\phi}(\mathbf{r}) = \frac{1}{\mu_0 M_s^2} \frac{1}{\sin \theta} \frac{\partial^2 E'(\mathbf{r})}{\partial \phi \partial \theta}. \quad (15c)$$

The second term in (15b) is required to make $h'_{\phi\phi}$ independent of the choice of coordinate system. With this term, the ϕ derivatives are effectively taken along a “great circle” path on the unit sphere rather than a constant- θ path. For this paper, however, this distinction is unimportant because we assume $\theta = \pi/2$.

The spatial dependence of the inhomogeneous perturbation energy is assumed to be described by a correlation function $C(R)$ defined by expressions of the form

$$\frac{1}{L^2} \int d\mathbf{r} h'_{\theta\theta}(\mathbf{r}) h'_{\phi\phi}(\mathbf{r} + \mathbf{R}) = \langle h'_{\theta\theta} h'_{\phi\phi} \rangle C(R) \quad (16)$$

where $\langle x \rangle$ indicates the expectation value of x , L^2 is the sample area, and \mathbf{r} and \mathbf{R} are vectors in the plane of the film. The sample is assumed to be macroscopically isotropic so that the correlation function depends only on the magnitude R . Because the stiffness fields are all derived from the same microstructure as represented by E' , correlations between different combinations of stiffness fields are assumed to be described by the same function $C(R)$.

The Fourier components of the perturbation stiffness fields can be characterized by the Fourier transform of (16)

$$\langle h'_{\theta\theta}(\mathbf{k}) h'_{\phi\phi}(\mathbf{k}) \rangle = L^2 \langle h'_{\theta\theta} h'_{\phi\phi} \rangle C(\mathbf{k}). \quad (17)$$

If the inhomogeneity has a characteristic length scale ξ , $C(\mathbf{k})$ is expected to become small for $k\xi \gg 1$.

The properties of spin waves presented in Section II and the statistical properties of the inhomogeneity given above are used here to describe the dynamic behavior of nearly uniform precession of the magnetization in an inhomogeneous thin film. The field due to inhomogeneities is given by

$$\mathbf{H}'(\mathbf{r}) = -\mathbf{h}'(\mathbf{r})\mathbf{m}(\mathbf{r}) \quad (18)$$

and in terms of Fourier components

$$\mathbf{H}'(\mathbf{q}) = - \int \frac{d\mathbf{k}}{(2\pi)^2} \mathbf{h}'(\mathbf{q} - \mathbf{k})\mathbf{m}(\mathbf{k}). \quad (19)$$

In the following, the amplitude of \mathbf{h}' is assumed small enough that only small nonuniformities are introduced into an otherwise uniform precession, i.e., that the $\mathbf{k} \neq 0$ spin-wave amplitudes are small compared with the amplitude of the $\mathbf{k} = 0$ mode. For an essentially uniform precession [illustrated in Fig. 3(a)]

$$\mathbf{m}(\mathbf{k}) = (2\pi)^2 \delta(\mathbf{k}) \frac{\mathbf{m}(\mathbf{k} = 0)}{L^2}. \quad (20)$$

Substituting this expression into (19), the inhomogeneous part of the effective field produced by the uniform precession interacting with the inhomogeneity [Fig. 3(b)] is given by

$$\mathbf{H}_{\text{eff}}(\mathbf{k})^{(0)} = -\mathbf{h}'(\mathbf{k}) \frac{\mathbf{m}(\mathbf{k} = 0)}{L^2} \quad (21)$$

and multiplication by the spin-wave susceptibility tensor $\chi_{\mathbf{k}}(\omega)$ gives spin-wave magnetization amplitude [Fig. 3(c)]

$$\mathbf{m}'(\mathbf{k}) = -\chi_{\mathbf{k}}(\omega) \mathbf{h}'(\mathbf{k}) \frac{\mathbf{m}(\mathbf{k} = 0)}{L^2}. \quad (22)$$

Each spin-wave mode will contribute to a uniform component of the effective field [Fig. 3(d)], so using (19) and (22), the uniform part of the field becomes

$$\begin{aligned} \mathbf{H}'(\mathbf{k} = 0) &= \left[\frac{1}{L^2} \int \frac{d\mathbf{k}}{(2\pi)^2} \mathbf{h}'^*(\mathbf{k}) \chi_{\mathbf{k}}(\omega) \mathbf{h}'(\mathbf{k}) \right] \mathbf{m}(\mathbf{k} = 0) \\ &\equiv \eta \mathbf{m}(\mathbf{k} = 0). \end{aligned} \quad (23)$$

Because the energy density is real, $h'_{ij}^*(\mathbf{k}) = h'_{ij}(-\mathbf{k})$. Equation (23) is the effective field acting on the uniform component of the magnetization due to spin waves excited through inhomogeneities. The total field experienced by the uniform mode is the sum of the $k = 0$ stiffness fields for the uniform film (8) and η , the effective stiffness field due to spin-wave excitation

$$\mathbf{H}(0) = -(\mathbf{h}_0 - \eta) \mathbf{m}(0). \quad (24)$$

Including the effects of spin-wave generation, the effective susceptibility to a uniform applied field is then rederived by replacing the stiffness tensor elements in (8) with the effective stiffness tensor $\mathbf{h}_0 - \eta$. The susceptibility becomes

$$\chi_0(\omega) = \frac{1}{Z'_0} \begin{bmatrix} h_{\phi\phi,0} - \eta_{\phi\phi} + i \frac{\alpha\omega}{\omega_M} & +\eta_{\theta\phi} + i \frac{\omega}{\omega_M} \\ +\eta_{\phi\theta} - i \frac{\omega}{\omega_M} & h_{\theta\theta,0} - \eta_{\theta\theta} + i \frac{\alpha\omega}{\omega_M} \end{bmatrix} \quad (25a)$$

with

$$Z'_0 = Z_0 + \frac{2\omega\delta\omega'_0}{\omega_M^2} \quad (25b)$$

where Z_0 is obtained from (10b). To lowest order in η , the resonant frequency is changed by an amount

$$\begin{aligned} \delta\omega'_0 &= -\frac{\omega_M^2}{2\omega} \left[\left(h_{\theta\theta,0} + i\alpha \frac{\omega}{\omega_M} \right) \eta_{\phi\phi} \right. \\ &\quad \left. + \left(h_{\phi\phi,0} + i\alpha \frac{\omega}{\omega_M} \right) \eta_{\theta\theta} - i \left(\frac{\omega}{\omega_M} \right) (\eta_{\theta\phi} - \eta_{\phi\theta}) \right]. \end{aligned} \quad (26)$$

Each of the elements of the η tensor contains an integral over \mathbf{k} on four terms, one for each element of the susceptibility tensor. For purposes of illustration, consider $\eta_{\theta\theta}$

$$\begin{aligned} \eta_{\theta\theta} &= \frac{1}{L^2} \int \frac{d\mathbf{k}}{(2\pi)^2} \\ &\quad \times \left[h'_{\theta\theta}^*(\mathbf{k}) \chi_{\theta\theta,\mathbf{k}} h'_{\theta\theta}(\mathbf{k}) + h'_{\theta\theta}^*(\mathbf{k}) \chi_{\theta\phi,\mathbf{k}} h'_{\phi\theta}(\mathbf{k}) \right. \\ &\quad \left. + h'_{\theta\phi}^*(\mathbf{k}) \chi_{\phi\theta,\mathbf{k}} h'_{\theta\theta}(\mathbf{k}) \right. \\ &\quad \left. + h'_{\phi\phi}^*(\mathbf{k}) \chi_{\phi\phi,\mathbf{k}} h'_{\phi\phi}(\mathbf{k}) \right]. \end{aligned} \quad (27)$$

Expanding η using (10) for the spin-wave susceptibility, $\delta\omega'_0$ can be written as

$$\begin{aligned} \delta\omega'_0 &= -\frac{\omega_M^2}{2\omega} \int \frac{d\mathbf{k}}{(2\pi)^2} \frac{C(\mathbf{k})}{Z_{\mathbf{k}}} \\ &\quad \times \left\{ 2 \frac{\omega^2}{\omega_M^2} \langle h'_{\theta\theta} h'_{\phi\phi} \rangle \right. \\ &\quad \left. + \left[h_{\phi\phi,0} h_{\phi\phi,\mathbf{k}} + \frac{i\alpha\omega}{\omega_M} (h_{\phi\phi,\mathbf{k}} + h_{\theta\theta,0}) \right] \langle h'_{\theta\theta}{}^2 \rangle \right. \\ &\quad \left. + \left[h_{\theta\theta,0} h_{\theta\theta,\mathbf{k}} + \frac{i\alpha\omega}{\omega_M} (h_{\theta\theta,\mathbf{k}} + h_{\phi\phi,0}) \right] \langle h'_{\phi\phi}{}^2 \rangle \right. \\ &\quad \left. + \left[h_{\theta\theta,0} h_{\phi\phi,\mathbf{k}} + h_{\phi\phi,0} h_{\theta\theta,\mathbf{k}} - 2 \frac{\omega^2}{\omega_M^2} + \frac{i\alpha\omega}{\omega_M} \right. \right. \\ &\quad \left. \left. \times (h_{\theta\theta,\mathbf{k}} + h_{\phi\phi,\mathbf{k}} + h_{\theta\theta,0} + h_{\phi\phi,0}) \right] \langle h'_{\theta\phi}{}^2 \rangle \right\} \end{aligned} \quad (28)$$

where terms of order α^2 have been dropped.

The imaginary parts of $\delta\omega'_0$ contribute to the linewidth so that the full-width at half-maximum in the imaginary part of the susceptibility is

$$\Delta\omega = \alpha\omega_M (h_{\theta\theta,0} + h_{\phi\phi,0}) + 2\text{Im}(\delta\omega'_0) \quad (29)$$

while the real part of $\delta\omega'_0$ is a shift in the resonant frequency.

Equation (28) for the complex frequency shift due to inhomogeneity is a primary result of this paper. The uniform film properties are described by the stiffness tensor elements ($h_{\theta\theta,\mathbf{k}}$, etc.) given in (8) and $Z_{\mathbf{k}}$ given in (10b). The properties of the inhomogeneity are described by the inhomogeneity stiffness tensor elements ($h'_{\theta\theta}$, etc.) given in (15) and with spatial information encoded in $C(\mathbf{k})$ (16). This classical result has a number of features in common with the quantum mechanical result. The expression includes a sum/integral over wave vectors and the perturbation strength appears quadratically as elements of \mathbf{h}' in (28) and as $A_{\mathbf{k}}$ in (13). Additionally, note that $|Z_{\mathbf{k}}|$ is minimum for frequencies $\omega_0 \approx \omega_{\mathbf{k}}$ so that degenerate spin-wave modes contribute most to the integral in (23). The quantum mechanical and classical descriptions differ in that spin waves with $\omega_{\mathbf{k}} \neq \omega_0$

and nonzero damping contribute somewhat because of the finite width of the spin-wave susceptibility maxima, where they are excluded in the quantum mechanical result.

V. ANALYTICAL APPROXIMATION

This section focuses on situations where the two-magnon contribution to the linewidth $\Delta\omega' = 2\text{Im}(\delta\omega'_0)$ may be calculated analytically. The methods used here closely follow Arias and Mills [38]. The principal conditions required to obtain analytical results include taking the limit of zero damping, film thickness less than the exchange length, and a cutoff length scale for the inhomogeneity. Because the effective damping is calculated at resonance, $\omega \approx \omega_0$.

The limit of zero damping allows one to take advantage of the fact that $\text{Im} Z_{\mathbf{k}}^{-1}$ is a peaked function centered at $\omega_0 = \omega_{\mathbf{k}}$ with width proportional to α . The limit of zero damping allows the approximation

$$\lim_{\alpha \rightarrow 0} \text{Im} \frac{-1}{Z_{\mathbf{k}}} \approx \frac{\pi\omega_M^2}{2\omega_0} \delta(\omega_{\mathbf{k}} - \omega_0). \quad (30)$$

Next, to evaluate the delta function in (30), the dispersion relation $\omega_{\mathbf{k}}$ is expanded for small values of k , specifically by approximating $N_k \approx 1 - kd/2$. This approximation is valid if $kd \ll 1$ and if the quadratic term in an expansion of $M_s N_k$ is small compared to Dk^2 , i.e., the film thickness d must be much smaller than the magnetostatic exchange length $l_{\text{ex}} = \sqrt{D/M_s}$, which is typically a few nanometers for most ferromagnetic transition metals. Using (8), the dispersion relation is approximated by

$$\left(\frac{\omega_{\mathbf{k}}}{\gamma}\right)^2 \approx \left(\frac{\omega_0}{\gamma}\right)^2 + a(\psi_{\mathbf{k}})k + bk^2 \quad (31a)$$

where

$$\left(\frac{\omega_0}{\gamma}\right)^2 = H_i(H_i + M_s \cos^2 \phi) \quad (31b)$$

$$a(\psi_{\mathbf{k}}) = [H_i(\sin^2 \psi_{\mathbf{k}} + \cos^2 \psi_{\mathbf{k}} \sin^2 \phi - \cos^2 \phi) + M_s \sin^2 \psi_{\mathbf{k}} \cos^2 \phi] M_s \frac{d}{2} \quad (31c)$$

$$b = (2H_i + M_s \cos^2 \phi)D. \quad (31d)$$

If $a(\psi_{\mathbf{k}})$ is negative, there will be real, positive values of k that give $\omega_{\mathbf{k}} = \omega_0$. A critical value of $\psi_{\mathbf{k}}$ is determined by $a(\psi_{\mathbf{k}}) = 0$

$$\sin^2 \psi_{\mathbf{k}}^{\text{crit}} = \frac{H_i \cos(2\phi)}{(H_i + M_s) \cos^2 \phi}. \quad (32)$$

Note that for magnetization angles $\phi > \pi/4$, there are no degenerate spin waves with solutions for real values of $\psi_{\mathbf{k}}$.

The largest wave number for which $\omega_{\mathbf{k}} = \omega_0$ is found for $\psi_{\mathbf{k}} = 0$

$$k^{\text{max}} = \frac{-a(0)}{b} = \frac{H_i \cos(2\phi) M_s d}{2D(2H_i + M_s \cos^2 \phi)}. \quad (33)$$

Next, the inhomogeneity is assumed to have a correlation length ξ such that the normalized perturbation stiffness fields have correlation functions such as

$$C(\mathbf{R}) = e^{-|\mathbf{R}|/\xi}. \quad (34)$$

The presence of a correlation length implies a high-wave-vector cutoff in the Fourier components of the perturbation fields

$$\langle h'_{\theta\theta}(\mathbf{k}) h'_{\phi\phi}(\mathbf{k}) \rangle = L^2 \langle h'_{\theta\theta}(\mathbf{r}) h'_{\phi\phi}(\mathbf{r}) \rangle \frac{2\pi\xi^2}{[1 + (k\xi)^2]^{3/2}}. \quad (35)$$

The final simplifying assumption in this section is that the uniform film stiffness fields may be replaced by their $k = 0$ values, e.g., that $h_{\theta\theta, \mathbf{k}}$ is not strongly k -dependent. This approximation is consistent with the assumption of an ultrathin film that was made above to obtain the quadratic expansion of the dispersion relation in (31a).

Incorporation of these approximations and assumptions leads to an intermediate result for the two-magnon linewidth

$$\Delta\omega' \approx \langle \delta\omega'_{\text{loc}}(\mathbf{r})^2 \rangle \int d\mathbf{k} \frac{\xi^2 \delta(\omega_{\mathbf{k}} - \omega_0)}{[1 + (k\xi)^2]^{3/2}} \quad (36)$$

where

$$\delta\omega'_{\text{loc}}(\mathbf{r}) = \frac{\omega_M^2}{2\omega_0} [h_{\phi\phi, 0} h'_{\theta\theta}(\mathbf{r}) + h_{\theta\theta, 0} h'_{\phi\phi}(\mathbf{r})] \quad (37)$$

is the local shift in resonance frequency due to inhomogeneity in the absence of interactions. This quantity differs from the local resonance linewidth in that a complete calculation of local resonance linewidth would account for the effects of E' on the equilibrium values of ϕ and θ .

A. Small Defect Limit

The small defect limit is defined by $\xi k^{\text{max}} \ll 1$. In this case, the perturbation stiffness fields are essentially independent of \mathbf{k} over the region of reciprocal space where the delta function is nonzero so the denominator in the integral in (36) is approximately unity. Integrating along the path described by $\omega_{\mathbf{k}} = \omega_0$, shown in Fig. 2(b)

$$\int d\mathbf{k} \delta(\omega_{\mathbf{k}} - \omega_0) = \oint \frac{\sqrt{k^2 + (\frac{dk}{d\psi_{\mathbf{k}}})^2} d\psi_{\mathbf{k}}}{|\nabla_{\mathbf{k}} \omega_{\mathbf{k}}|} = \frac{8\omega_0}{\gamma^2 b} \psi_{\mathbf{k}}^{\text{crit}}. \quad (38)$$

This approximation yields an analytical expression for the two-magnon part of the linewidth in the small defect limit

$$\Delta\omega'_{\text{sm}} \approx 4\psi_{\mathbf{k}}^{\text{crit}} \frac{\langle \delta\omega'_{\text{loc}}(\mathbf{r})^2 \rangle}{\delta\omega_{\text{ex}}} \quad (39)$$

where

$$\delta\omega_{\text{ex}} = \frac{D}{2\omega\xi^2} \gamma^2 (2H_i + M_s \cos^2 \phi) \quad (40)$$

is the difference between the frequency of uniform precession and the frequency of a spin wave with $k = 1/\xi$ due to exchange interactions alone. In the small defect limit, the local resonance frequency variations are narrowed by both the exchange interactions and by the magnetostatic interactions that determine the ellipticity of the precession and $\psi_{\mathbf{k}}^{\text{crit}}$.

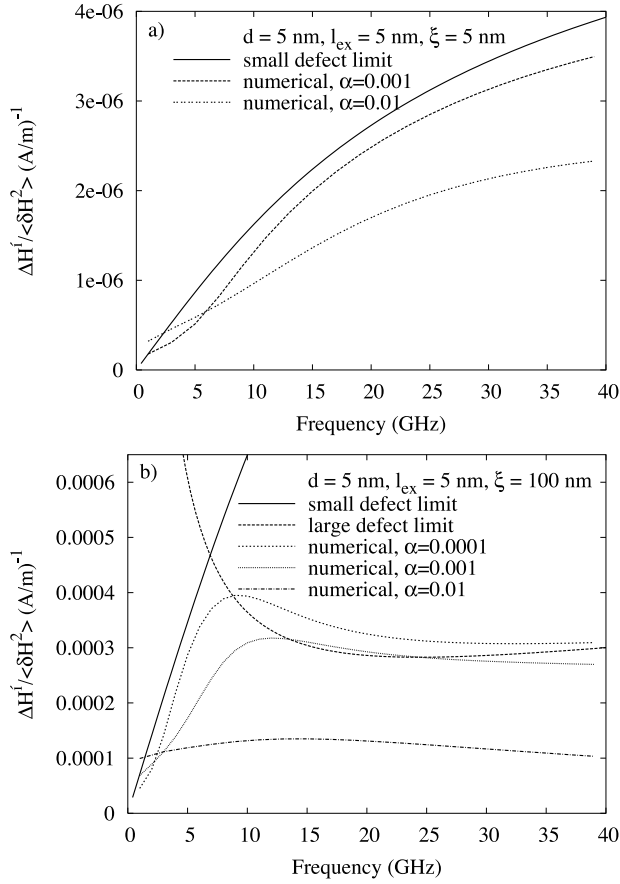


Fig. 4. Two-magnon contribution to the field linewidth as a function of frequency for two sizes of defects: (a) $\xi = 5$ nm, and (b) $\xi = 100$ nm. In (a), the large defect limit would be off scale.

B. Large Defect Limit

In the large defect limit, where $\xi k^{\text{max}} \gg 1$, the upper limit of the integral over wave vectors in (36) is effectively determined by the defect correlation length ξ . Integrating along four small- k segments where $\sin^2(\psi_{\mathbf{k}}) = \sin^2(\psi_{\mathbf{k}}^{\text{crit}})$

$$\int d\mathbf{k} \frac{\delta(\omega_{\mathbf{k}} - \omega_0)}{[1 + (k\xi)^2]^{3/2}} \approx 4 \int_0^\infty \frac{dk}{|\nabla_{\mathbf{k}} \omega_{\mathbf{k}}| [1 + (k\xi)^2]^{3/2}} = \frac{8\omega_0}{\xi\gamma^2} \left| \frac{da}{d\psi_{\mathbf{k}}} \right|_{\psi_{\mathbf{k}}^{\text{crit}}}^{-1}. \quad (41)$$

Incorporation of this result yields an analytical expression for the two-magnon linewidth in the large defect limit

$$\Delta\omega'_{\text{lg}} \approx 16 \frac{\omega_0 \xi}{\omega_M d \gamma (H_i + M_s) \cos^2(\phi) \sin(2\psi_{\mathbf{k}}^{\text{crit}})} \langle \delta\omega'_{\text{loc}}(\mathbf{r})^2 \rangle. \quad (42)$$

In the large defect limit, the spread in local resonance frequencies is narrowed by magnetostatic interactions, both through $\psi_{\mathbf{k}}^{\text{crit}}$ and explicitly through $\xi/\omega_M d$.

C. Unit Conversion

The derivations and results above are presented in SI units. For those who prefer cgs units, the following conversions are needed. In (8), (39), and (42), M_s (SI) should be replaced by $4\pi M_s$ (cgs). Normalization of the stiffness fields in (8) by $4\pi M_s$ allows these unitless quantities to have the same

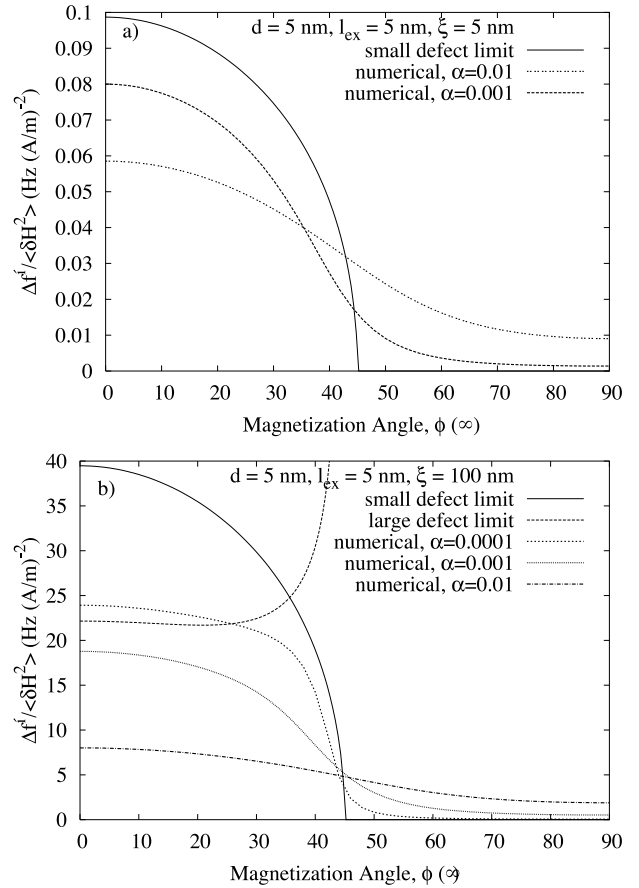


Fig. 5. Two-magnon contribution to the frequency linewidth as a function of angle at 10 GHz for (a) small defects, $\xi = 5$ nm, and (b) large defects, $\xi = 100$ nm. The magnetization is in plane at 0° . In (a), the large defect limit is off scale.

numerical value in both unit systems. Also, $\omega_M = |\gamma| M_s$ (SI) has the same numerical value as $|\gamma| 4\pi M_s$ (cgs) with $|\gamma| = 17.6 \times 10^6 \text{ G}^{-1} \text{ s}^{-1}$. Finally, the perturbation stiffness fields in (15) are converted by replacing μ_0 with 4π .

VI. EXAMPLE CALCULATIONS

This section presents example calculations where the inhomogeneity consists of an inhomogeneous applied magnetic field $\delta H(\mathbf{r})$ that is collinear with the magnetization, but that varies in strength and sign as a function of position such that (34) and (35) are valid. In some sense, such a field is unphysical, but it is helpful for purposes of illustration. Statistical properties of other, perhaps more realistic types of inhomogeneity are presented in Appendix I. For the simple inhomogeneous applied field

$$h'_{\theta\theta}(\mathbf{r}) = h'_{\phi\phi}(\mathbf{r}) = \frac{\delta H(\mathbf{r})}{M_s} \quad (43a)$$

$$h'_{\theta\phi}(\mathbf{r}) = 0. \quad (43b)$$

The two-magnon contribution to the linewidth is calculated using the analytical results for the small defect limit (39) and the large defect limit (42) in addition to numerical evaluations of (28) for different values of the damping parameter α . In Fig. 4, the two-magnon contributions to the field linewidth are presented as a function of frequency for two values of ξ with the

TABLE I
EXPECTATION VALUES OF INHOMOGENEITY STIFFNESS FIELDS FOR A VARIETY OF POSSIBLE INHOMOGENEOUS PERTURBATION ENERGY TERMS

| Type | | $\frac{(\mu_0 M_s^2)^2}{K^2} \langle h'_{\theta\theta} \rangle$ | $\frac{(\mu_0 M_s^2)^2}{K^2} \langle h'_{\phi\phi} \rangle$ | $\frac{(\mu_0 M_s^2)^2}{K^2} \langle h'_{\theta\phi} \rangle$ | $\frac{(\mu_0 M_s^2)^2}{K^2} \langle h'_{\theta\theta} h'_{\phi\phi} \rangle$ |
|--------------------------------|---------------------------------------------|-----------------------------------------------------------------|-------------------------------------------------------------|---------------------------------------------------------------|-------------------------------------------------------------------------------|
| Random Field ^a | $K(\hat{\mathbf{m}} \cdot \mathbf{p}')$ | $\frac{1}{3}$ | $\frac{1}{3}$ | 0 | $\frac{1}{3}$ |
| Normal Uniaxial | $K'(\hat{\mathbf{m}}_y)^2$ | $4 \sin^4 \phi$ | $4 \cos^2(2\phi)$ | 0 | $-4 \sin^2 \phi \cos(2\phi)$ |
| In-plane Uniaxial ^b | $K(\hat{\mathbf{m}} \cdot \mathbf{u}')^2$ | $\frac{3}{2} - \cos^2 \phi + \frac{3}{2} \cos^4 \phi$ | $\frac{3}{2} \cos^2(2\phi)$ | $\frac{1}{2} \sin^2 \phi$ | $\frac{1}{2} [3 \cos^2 \phi - 1] \cos(2\phi)$ |
| Random Uniaxial ^b | $K(\hat{\mathbf{m}} \cdot \mathbf{p}')^2$ | $\frac{16}{15}$ | $\frac{16}{15}$ | $\frac{4}{15}$ | $\frac{8}{15}$ |
| K_2 Uniaxial ^b | $K(\hat{\mathbf{m}} \cdot \mathbf{p}')^4$ | $\frac{512}{315}$ | $\frac{512}{315}$ | $\frac{16}{35}$ | $\frac{32}{45}$ |
| K_1 Cubic | ^c | $\frac{116}{105}$ | $\frac{116}{105}$ | $\frac{12}{188}$ | $\frac{44}{212}$ |
| K_2 Cubic | $K(\hat{m}_{x'}\hat{m}_{y'}\hat{m}_{z'})^2$ | $\frac{28}{715}$ | $\frac{28}{715}$ | $\frac{35}{15015}$ | $\frac{105}{15015}$ |

a \mathbf{p}' is a unit vector with random direction.

b \mathbf{u}' is a unit vector with random direction in the plane of the film.

c $K \left[(\hat{m}_{x'}\hat{m}_{y'})^2 + (\hat{m}_{y'}\hat{m}_{z'})^2 + (\hat{m}_{z'}\hat{m}_{x'})^2 \right]$

field and magnetization applied in plane. In this orientation, the field linewidth is related to the frequency linewidth by

$$\gamma^2(2H_i + M)\Delta H' = 2\omega\Delta\omega'. \quad (44)$$

For low frequencies and magnetization in plane, the internal field H_i becomes small, and according to (33), the maximum degenerate spin-wave wave vector also becomes small, so that the small defect limit will be reached in the limit of low frequencies. This behavior is illustrated in Fig. 4(b), where the numerical results approach the small defect limit for low frequencies and approach the large defect limit for high frequencies.

In Fig. 5, the angular dependence of the two-magnon contribution to the frequency linewidth is plotted for two values of ξ . For arbitrary applied field direction, the magnetization is not generally parallel to the applied field, and the simple conversion from frequency linewidth to field linewidth in (44) is not applicable.

As the magnetization angle ϕ approaches 45° , (33) shows that the maximum degenerate spin-wave wave vector goes to zero, so that while the large defect limit may be appropriate when the magnetization is in plane, the small defect limit will be approached as $\phi \rightarrow 45^\circ$.

For $\phi > 45^\circ$, there are no degenerate spin waves and the analytical results in the zero damping limit predict zero two-magnon linewidth in this range. For finite damping, however, spin waves may be excited off resonance, and the numerical calculation yields a finite two-magnon linewidth.

VII. DISCUSSION

In addition to the description of the two-magnon linewidth as an active process, where defects drive spin waves or defects scatter magnons, it is also productive to think of the two-magnon linewidth in a more passive sense as the apparent resonance variation that remains after local resonances have been coupled and essentially averaged by exchange and dipolar interactions [18], [52]. In this passive description, it is clear that the two-magnon linewidth must be less than the local variations in the resonance condition in the absence of interactions, i.e., $\Delta H'$ must be smaller than the local effective field variation and $\Delta\omega'$ must be smaller than the corresponding change in resonance frequency due to the local effective field variation.

In both this classical model and the quantum mechanical version, the derivation is through a perturbation approach, and it is important to recognize that this fact places limits on the validity of the results, but it is not immediately clear what these limits are. The dependence of the linewidth on defect size and defect strength offer some indications. Both analytical two-magnon results presented above increase with increasing defect size and quadratically with defect strength, but the linewidth cannot be increased without limit. It has been recently demonstrated that for increasing defect size, the linewidth reaches a maximum value corresponding to the local resonance model [18]. Using Fig. 4, 100 kA/m (1.2 kOe) rms field fluctuations correlated over $\xi = 5$ nm and $\alpha = 0.01$ would broaden the resonance line by approximately 10 kA/m (120 Oe) [Fig. 4(a)]. For $\xi = 100$ nm, and fluctuations with the same amplitude, however, the two-magnon model would predict an absurd two-magnon line broadening of approximately 1.3 MA/m, and the local resonance model would be more accurate.

Although the two-magnon model and its classical analog yield effective damping rates, it should be noted that they are *apparent* damping rates only in the context of ferromagnetic resonance experiments, that they do not describe real damping in the sense of coupling to the thermal bath.

Comparison of the analytical results, (39) and (42) in the zero damping limit with numerical results calculated from (28) shows that the damping modifies the two-magnon linewidth significantly for damping parameter values typical of magnetic metals. The analytical results may not be sufficiently accurate for all purposes of fitting experimental data, but they do provide useful estimates of the two-magnon linewidth.

APPENDIX STATISTICS FOR POLYCRYSTALS

The main results of this paper, the effective frequency shift (28) and the analytical linewidth expressions (39) and (42), are written in a form that is independent of the microstructural origins of the inhomogeneity. To calculate linewidths for a particular form of inhomogeneity, estimates of $C(\mathbf{k})$ or the correlation length ξ must be made, and the expectation values $\langle h'_{\theta\theta} h'_{\phi\phi} \rangle$, etc., must be calculated from the symmetry properties of the inhomogeneity. The example calculations in Section VI are for a very simple form of inhomogeneity, a random strength ap-

plied field. For a number of more complicated types of inhomogeneity, Table I lists expectation values of inhomogeneity stiffness fields for a variety of possible inhomogeneous perturbation energy terms.

The method used to calculate these values is outlined here. The normalized magnetization vector in the laboratory frame, $\hat{m}_{\text{lab}} = (\sin \theta \cos \phi, \sin \theta \sin \phi, \cos \theta)$, is expressed in the coordinates of the local crystallographic axes using a rotation matrix $R(\alpha, \beta, \gamma)$ that depends on Euler angles α , β , and γ

$$\hat{m}_{\text{loc}} = R(\alpha, \beta, \gamma) \hat{m}_{\text{lab}}. \quad (45)$$

For each form of anisotropy, the local anisotropy energy can be expressed simply in terms of \hat{m}_{loc} and expanded in terms of \hat{m}_{lab} . The resulting complicated expression is differentiated with respect to θ and ϕ via (15) to obtain stiffness fields. The expectation values are then obtained by integrating products of these stiffness fields over the Euler angles.

ACKNOWLEDGMENT

The authors would like to thank A. Kunz and D. Twisselmann for their assistance and J. Warren, M. Stiles, and C. Patton for their helpful comments.

REFERENCES

- [1] V. L. Safonov, "Tensor form of magnetization damping," *J. Appl. Phys.*, vol. 91, pp. 8653–8655, 2002.
- [2] V. L. Safonov and H. N. Bertram, "Linear stochastic magnetization dynamics and microscopic relaxation mechanisms," *J. Appl. Phys.*, vol. 94, pp. 529–538, 2003.
- [3] N. Smith, "Fluctuation-dissipation considerations for phenomenological damping models for ferromagnetic thin films," *J. Appl. Phys.*, vol. 92, no. 7, pp. 3877–3885, 2002.
- [4] V. Kamberský and C. E. Patton, "Spin-wave relaxation and phenomenological damping in ferromagnetic resonance," *Phys. Rev. B, Condens. Matter*, vol. 11, pp. 2668–2672, 1975.
- [5] V. Kamberský, "On the Landau–Lifshitz relaxation in ferromagnetic metals," *Can. J. Phys.*, vol. 48, pp. 2906–2911, 1970.
- [6] V. Korenman and R. E. Prange, "Anomalous damping of spin waves in magnetic metals," *Phys. Rev. B, Condens. Matter*, vol. 6, pp. 2769–2777, 1972.
- [7] L. Berger, "A simple theory of spin-wave relaxation in ferromagnetic metals," *J. Phys. Chem. Solids*, vol. 38, pp. 1321–1326, 1977.
- [8] V. L. Safonov and H. N. Bertram, "Impurity relaxation mechanism for dynamic magnetization reversal in a single domain grain," *Phys. Rev. B, Condens. Matter*, vol. 61, pp. 14 893–14 896, 2000.
- [9] S. E. Russek, P. Kabos, R. D. McMichael, C. G. Lee, W. E. Bailey, R. Ewasko, and S. C. Sanders, "Magnetostriction and angular dependence of ferromagnetic resonance linewidth in Tb-doped $\text{Ni}_{0.8}\text{Fe}_{0.2}$ thin films," *J. Appl. Phys.*, vol. 91, pp. 8659–8661, 2002.
- [10] N. Smith and P. Arnett, "White-noise magnetization fluctuations in magnetoresistive heads," *Appl. Phys. Lett.*, vol. 78, pp. 1448–1450, 2001.
- [11] H. N. Bertram, Z. Jin, and V. Safonov, "Experimental and theoretical studies of thermal magnetization noise in GMR heads," *IEEE Trans. Magn.*, vol. 38, pp. 38–44, Jan. 2002.
- [12] H. N. Bertram, V. L. Safonov, and Z. Jin, "Thermal magnetization noise, damping fundamentals and mode analysis: Application to a thin film GMR sensor," *IEEE Trans. Magn.*, vol. 38, pp. 2514–2519, Sept. 2002.
- [13] V. L. Safonov and H. N. Bertram, "Thermal magnetization noise in a thin film," *Phys. Rev. B, Condens. Matter*, vol. 65, pp. 172 417–172 417, 2002.
- [14] —, "Nonuniform thermal magnetization noise in thin films: Application to GMR heads," *J. Appl. Phys.*, vol. 91, pp. 7279–7281, 2002.
- [15] T. J. Silva, C. S. Lee, T. M. Crawford, and C. T. Rogers, "Inductive measurement of ultrafast magnetization dynamics in thin-film Permalloy," *J. Appl. Phys.*, vol. 85, pp. 7849–7862, 1999.
- [16] C. E. Patton, "Microwave resonance and relaxation," in *Magnetic Oxides*, D. J. Craik, Ed. London, U.K.: Wiley, 1975, ch. 10, pp. 575–648.
- [17] D. J. Twisselmann and R. D. McMichael, "Intrinsic damping and intentional ferromagnetic resonance broadening in thin Permalloy films," *J. Appl. Phys.*, vol. 93, pp. 6903–6905, 2003.
- [18] R. D. McMichael, D. J. Twisselmann, and A. Kunz, "Localized ferromagnetic resonance in inhomogeneous thin films," *Phys. Rev. Lett.*, vol. 90, pp. 227 601–227 601, 2003.
- [19] E. Schlömann, "Inhomogeneous broadening of ferromagnetic resonance lines," *Phys. Rev.*, vol. 182, pp. 632–645, 1969.
- [20] —, "Ferromagnetic resonance in polycrystals," *J. Phys. Radium*, vol. 20, pp. 327–332, 1959.
- [21] E. Schlömann and J. R. Zeender, "Ferromagnetic resonance in polycrystalline nickel ferrite aluminate," *J. Appl. Phys.*, vol. 29, pp. 341–341, 1958.
- [22] E. Schlömann and R. V. Jones, "Ferromagnetic resonance in polycrystalline ferrites with hexagonal crystal structure," *J. Appl. Phys.*, vol. 30, pp. 1775–1785, 1959.
- [23] E. Schlömann, "Ferromagnetic resonance in polycrystalline ferrites with large anisotropy—I. General theory and application to cubic materials with a negative anisotropy constant," *J. Phys. Chem. Solids*, vol. 6, pp. 257–266, 1958.
- [24] W. Anders and E. Biller, "Ferromagnetic resonance linewidth in bulk nickel for various angles between the static field and the surface of the sample," *J. Phys., Colloque*, vol. 32, pp. C1-774–776, 1971.
- [25] C. Chappert, K. L. Dang, P. Beauvillain, H. Hurdequint, and D. Renard, "Ferromagnetic resonance studies of very thin cobalt films on a gold substrate," *Phys. Rev. B, Condens. Matter*, vol. 34, pp. 3192–3197, 1986.
- [26] W. Platow, A. N. Anisimov, G. L. Dunifer, M. Farle, and K. Baberschke, "Correlations between ferromagnetic-resonance linewidths and sample quality in the study of metallic ultrathin films," *Phys. Rev. B, Condens. Matter*, vol. 58, pp. 5611–5621, 1998.
- [27] S. Mizukami, Y. Ando, and T. Miyazaki, "The study on ferromagnetic resonance linewidth for NM/80NiFe/NM (NM = Cu, Ta, Pd and Pt) films," *Jpn. J. Appl. Phys.*, vol. 40, pp. 580–585, 2001.
- [28] —, "Ferromagnetic resonance linewidth for NM/80NiFe/NM films (NM = Cu, Ta, Pd and Pt)," *J. Magn. Magn. Mater.*, vol. 226–230, pp. 1640–1642, 2001.
- [29] B. Heinrich and J. F. Cochran, "FMR linebroadening in metals due to two-magnon scattering," *J. Appl. Phys.*, vol. 57, pp. 3690–3692, 1985.
- [30] Z. Celinski and B. Heinrich, "Ferromagnetic resonance linewidth of Fe ultrathin films grown on a bcc Cu substrate," *J. Appl. Phys.*, vol. 70, pp. 5935–5937, 1991.
- [31] C. E. Patton and C. H. Wilts, "Temperature dependence of the ferromagnetic resonance linewidth in thin Ni-Fe films," *J. Appl. Phys.*, vol. 38, pp. 3537–3540, 1967.
- [32] L. Kraus, Z. Frait, and J. Schneider, "Ferromagnetic resonance in amorphous $\text{FeNi}_{80}\text{P}_{10}\text{B}_{10}$ alloys," *Phys. Stat. Sol.*, vol. 64, pp. 449–456, 1981.
- [33] M. L. Spano and S. M. Bhagat, "Ferromagnetic resonance in amorphous alloys," *J. Magn. Magn. Mater.*, vol. 24, pp. 143–156, 1981.
- [34] T. D. Rosing, "Resonance linewidth and anisotropy variation in thin films," *J. Appl. Phys.*, vol. 34, pp. 995–995, 1963.
- [35] Q. H. F. Vrehen, "Absorption and dispersion in porous and anisotropic polycrystalline ferrites at microwave frequencies," *J. Appl. Phys.*, vol. 40, pp. 1849–1860, 1969.
- [36] Q. H. F. Vrehen, A. B. van Groenou, and J. G. M. de Lau, "Relaxation of ferromagnetic precession by excitation of spin-waves in a polycrystalline ferrite," *Solid State Commun.*, vol. 7, pp. 117–121, 1969.
- [37] A. M. Clogston, "Inhomogeneous broadening of magnetic resonance lines," *J. Appl. Phys.*, vol. 29, pp. 334–336, 1958.
- [38] R. Arias and D. L. Mills, "Extrinsic contributions to the ferromagnetic resonance response of ultrathin films," *Phys. Rev. B, Condens. Matter*, vol. 60, no. 10, pp. 7395–7409, 1999.
- [39] —, "Extrinsic contributions to the ferromagnetic resonance response of ultrathin films," *J. Appl. Phys.*, vol. 87, no. 9, pp. 5455–5456, 2000.
- [40] M. Sparks, "Ferromagnetic resonance in thin films. II. Theory of linewidths," *Phys. Rev. B, Condens. Matter*, vol. 1, pp. 3856–3869, 1970.
- [41] M. J. Hurben and C. E. Patton, "Theory of two magnon scattering microwave relaxation and ferromagnetic resonance linewidth in magnetic thin films," *J. Appl. Phys.*, vol. 83, no. 8, pp. 4344–4365, 1998.
- [42] R. D. McMichael, M. D. Stiles, P. J. Chen, and W. F. Egelhoff, Jr., "Ferromagnetic resonance linewidth in thin films coupled to NiO," *J. Appl. Phys.*, vol. 83, no. 11, pp. 7037–7039, 1998.
- [43] B. A. Kalinikos and A. N. Slavin, "Theory of dipole-exchange spin wave spectrum for ferromagnetic films with mixed exchange boundary conditions," *J. Phys. C, Solid State Phys.*, vol. 19, pp. 7013–7033, 1986.

- [44] K. J. Harte, "Theory of magnetization ripple in ferromagnetic films," *J. Appl. Phys.*, vol. 39, no. 3, pp. 1503–1524, 1968.
- [45] A. M. Clogston, H. Suhl, L. R. Walker, and P. W. Anderson, "Ferromagnetic resonance line width in insulating materials," *J. Phys. Chem. Solids*, vol. 1, pp. 129–136, 1956.
- [46] E. Schlömann, "Spin-wave analysis of ferromagnetic resonance in polycrystalline ferrites," *J. Phys. Chem. Solids*, vol. 6, pp. 242–256, 1958.
- [47] M. Sparks, R. Loudon, and C. Kittel, "Ferromagnetic relaxation. I. Theory of the relaxation of the uniform precession and the degenerate spectrum in insulators at low temperatures," *Phys. Rev.*, vol. 122, no. 3, pp. 791–803, 1961.
- [48] J. F. Cochran, R. W. Qiao, and B. Heinrich, "Two-magnon contribution to the ferromagnetic resonance linewidth in amorphous ferromagnetic metals," *Phys. Rev. B, Condens. Matter*, vol. 39, pp. 4399–4408, 1989.
- [49] H. B. Callen, *Fluctuation, Relaxation and Resonance in Magnetic Systems*. Edinburgh, U.K.: Oliver & Boyd, 1962, ch. 4, pp. 69–85.
- [50] C. W. Haas and H. B. Callen, "Ferromagnetic relaxation and resonance line widths," in *Magnetism*. New York: Academic, 1963, vol. 1, ch. 10, pp. 480–497.
- [51] M. Sparks, *Ferromagnetic Relaxation Theory. Advanced Physics Monograph Series*. New York: McGraw-Hill, 1964.
- [52] S. Geschwind and A. M. Clogston, "Narrowing effect of dipole forces on inhomogeneously broadened lines," *Phys. Rev.*, vol. 108, no. 1, pp. 49–53, 1957.

Robert D. McMichael (M'92) received the B.S. degree in engineering-physics from Pacific Lutheran University, Tacoma, WA, in 1985 and the M.S. and Ph.D. degrees from The Ohio State University, Columbus, in 1990.

Following a National Research Council Postdoctoral Associateship, he has continued as a Physicist in the Metallurgy Division at the National Institute of Standards and Technology, Gaithersburg, MD. His research interests include ferromagnetic resonance, magnetization dynamics, thin-film magnetism, exchange bias, giant magnetoresistance, and micromagnetic modeling.

Pavol Krivosik graduated in solid state physics in 1994 and received the Ph.D. degree in 2001 from the Faculty of Electrical Engineering, Slovak University of Technology, Bratislava, Slovakia.

At present, he is a Postdoctoral Associate in the Department of Physics, Colorado State University, Fort Collins. His research activities concern ferromagnetic resonance and linear and nonlinear magnetization dynamics in thin films.